

Nonlocal strain-softening model of quasi-brittle materials using boundary element method

Feng-Bao Lin^{a,*}, Geng Yan^b, Zdeněk P. Bažant^c, Fangming Ding^b

^aDepartment of Civil Engineering, Polytechnic University, 6 Metrotech Center, Brooklyn, NY 11201, USA

^bDepartment of Urban Construction, Suzhou Institute of Urban Construction and Environmental Protection, Suzhou, Jiangsu, People's Republic of China

^cDepartment of Civil Engineering and Materials Science, Northwestern University, Evanston, IL 60208, USA

Received 8 October 2000; revised 30 April 2001; accepted 17 October 2001

Abstract

The strain-softening localization problems have been studied intensively using the finite element methods. This paper addresses the localization using the boundary element approach. A plasticity model with yield limit degradation is implemented in a boundary element program to study the fracture behavior of quasi-brittle materials. A special integration algorithm is formulated and applied to deal with the singular integrations encountered in the volume integrals over the internal cells where strain-softening occurs. Strain-softening damage localizations are investigated. It is found that as different cell meshes are used in the analysis, the strain-softening region tends to localize into a zone of one cell width, which leads to incorrect results. A nonlocal strain-softening localization limiter is incorporated into the boundary element analysis to avoid the localization problems and attain realistic results. © 2002 Elsevier Science Ltd. All rights reserved.

Keywords: Nonlocal formulation; Boundary element method; Strain-softening; Quasi-brittle materials; Plasticity; Yield limit degradation

1. Introduction

It is generally recognized that the classical linear elastic fracture mechanics cannot be applied to heterogeneous (quasi-brittle) materials such as concrete, ceramics, composites, sea ice, etc. due to the existence of a fracture process zone which consists of a large number of microcracks in front of the crack tip. To simulate the fracture behavior of heterogeneous materials, smeared cracking models with strain-softening such as Bažant's crack band model or discrete-cracking models such as Hillerborg's fictitious crack model may be used [4,5,9,17,18].

Strain-softening is a phenomenon that reflects micro-cracking on the macrolevel in which the tangential moduli matrix of the material loses positive-definiteness. The stresses in a strain-softening material reduce gradually with the increasing of strains due to the growing of micro-cracks and finally reduce to zero as the microcracks develop into a major visible crack.

Difficulties have been experienced in a finite element analysis involving strain-softening damage behavior. As different meshes are used in the analysis, different results are obtained. The results are not objective with respect to the

finite element mesh refinements. When the mesh size is refined to zero, the material failure may happen with no energy dissipation because of the possibility of strain-softening localization into a zone of vanishing volume [4,5,7,8,9,16]. To remedy the problems associated with the strain-softening localization, Pijaudier-Cabot and Bažant [25] and Bažant et al. [11] postulated a nonlocal localization limiter to restrict the softening region to have a certain finite size which is considered as a material property. Later, Bažant and Lin [9] further developed a nonlocal continuum model with yield limit degradation and successfully avoided the problems of convergence at finite element mesh refinement and the spurious mesh sensitivity. Although more sophisticated nonlocal models have been developed subsequently [6,12,13,19,24], the model of Bažant and Lin [9] is adopted in this study for incorporation into the boundary element method.

The boundary element method, a comparatively new powerful numerical analysis method which transforms the governing differential equations of the solid under consideration to the corresponding boundary integral equations, possesses several advantages over the finite element method. One of the major advantages of the boundary element method is to reduce tremendously the number of unknown quantities by discretizing only the boundary of the solid rather than the entire domain. Thus, a great amount of

* Corresponding author. Tel.: +1-718-260-3676.

E-mail address: flin@poly.edu (F.-B. Lin).

time needed for preparing the input data and the computer running time can be saved. For the numerical analysis of strain-softening localization problems, because strain-softening tends to localize into a small region in the solid, the internal cells required for nonlinear regions are needed only in this small region rather than the entire domain of the solid.

Quite a number of studies [1–3,14,15,22,28,29] on the boundary element analysis of nonlinear elastoplastic problems have appeared since the first paper on the problem published in 1971 by Swedlow and Cruse [27]. However, the numerical analyses of strain-softening damage behavior have been limited to the finite element methods. The strain-softening localization problems have so far escaped attention of the researchers in boundary elements. An exception is a study of Lin and Yan [20] who applied the boundary element method to analyse the fracture process of heterogeneous materials using a strain-softening damage model. In this initial study, they found that the boundary element results appear to be unobjective with respect to the cell mesh refinements even though the nature of cells, which just serve for the purpose of carrying out the volume integration, is totally different from that of finite elements.

In this paper, a plasticity model with yield limit degradation is incorporated into a relatively simple classical version of the boundary element method to investigate strain-softening localization. The initial stress boundary element approach is applied to deal with the nonlinear strain-softening problems. A special semi-analytical integration method for triangular cells is used to carry out the volume integration over the cell that contains a singular node. The nonlocal formulation is also integrated into the boundary element program in order to overcome the difficulties associated with the strain-softening localization. A step-by-step iteration procedure with nonlocal treatment is presented. To verify if the nonlocal formulation can remedy the strain-softening localization problems, a rectangular panel with three different cell meshes is analyzed. The results obtained from local and nonlocal boundary element analyses are compared and presented. In a separate study [26], a nonlocal plasticity model is incorporated into a more sophisticated version of the boundary element method, in which regularized integral representations and boundary integral equations avoid the difficulties associated with the numerical computation of singular integrals, and further examples are presented.

2. Boundary element formulation for elastoplastic analysis

For elastoplastic problems based on small strain theory, the basic equations in incremental form are as follows [21,23]. The governing equations are

$$d\sigma_{ij,j} + db_i = 0 \tag{1}$$

with the boundary conditions

$$\begin{aligned} du_i(x) &= d\bar{u}_i(x) \quad x \in \Gamma_1, \\ d\tau_i(x) &= d\bar{\tau}_i(x) \quad x \in \Gamma_2, \quad \Gamma_1 + \Gamma_2 = \Gamma \end{aligned} \tag{2}$$

and the total strain increment is

$$d\varepsilon_{ij} = d\varepsilon_{ij}^e + d\varepsilon_{ij}^p = (du_{i,j} + du_{j,i})/2 \tag{3}$$

where $d\varepsilon_{ij}^e$ and $d\varepsilon_{ij}^p$ are the elastic and plastic strain increments, Γ the boundary of solid Ω under consideration, $d\sigma_{ij}$, db_i , du_i , and $d\tau_i$ the stress, body force (per unit volume), displacement, and traction increments, respectively, and $d\bar{u}_i$ and $d\bar{\tau}_i$ are prescribed displacements and prescribed tractions on boundary Γ_1 and Γ_2 , respectively. The yield criterion is

$$F(\sigma_{ij}, \kappa) = f(\sigma_{ij}) - \psi(\kappa) = 0 \tag{4}$$

where F and f are yield functions, ψ a work hardening function, and κ is the work hardening parameter. The constitutive equations are

$$\begin{aligned} d\sigma_{ij} &= D_{ijkl} d\varepsilon_{kl}^e = D_{ijkl}(d\varepsilon_{kl} - d\varepsilon_{kl}^p) = d\sigma_{ij}^e - d\sigma_{ij}^p \\ &= D_{ijkl}^{ep} d\varepsilon_{kl} \end{aligned} \tag{5}$$

where

$$D_{ijkl} = [2\mu\nu/(1 - 2\nu)]\delta_{ij}\delta_{kl} + \mu(\delta_{ik}\delta_{jl} + \delta_{il}\delta_{jk}),$$

$$D_{ijkl}^{ep} = D_{ijkl} - D_{ijmn}a_{mn}a_{op}D_{opkl}/\gamma,$$

$$\gamma = a_{ij}D_{ijkl}a_{kl} + (d\psi/d\kappa)\sigma_{ij}a_{ij}, \quad a_{ij} = (\partial F/\partial \sigma_{ij}) = \partial f/\partial \sigma_{ij}$$

Here $d\sigma_{ij}^e$ is the stress increment corresponding to $d\varepsilon_{ij}$ assuming elastic response, $d\sigma_{ij}^p$ equals $D_{ijkl} d\varepsilon_{kl}^p$ which adjusts the stress increment $d\sigma_{ij}^e$ to the actual stress increment, μ the shear modulus, and ν is Poisson's ratio.

Similar to the elasticity problems, the initial stress boundary integral equations for elastoplastic problems and the formulas for internal stresses can be found from Kelvin's solution and Betti's reciprocal theorem as:

$$c_{ij} du_j + \int_{\Gamma} T_{ij} du_j d\Gamma = \int_{\Gamma} U_{ij} d\tau_j d\Gamma + \int_{\Omega} E_{jki} d\sigma_{jk}^p d\Omega \tag{6}$$

$$\begin{aligned} d\sigma_{ij} &= \int_{\Gamma} V_{ijk} d\tau_k d\Gamma - \int_{\Gamma} S_{ijk} du_k d\Gamma \\ &+ \int_{\Gamma} F_{ijkl} d\sigma_{kl}^p d\Omega + f_{ij} \end{aligned} \tag{7}$$

where for two-dimensional plane strain problems

$$U_{ij} = c_1[-(3 - 4\nu)\delta_{ij} \ln(r) + r_{,i}r_{,j}],$$

$$T_{ij} = (c_2/r)\{(dr/dn)[(1 - 2\nu)\delta_{ij} + 2r_{,i}r_{,j}] - (1 - 2\nu)(n_{,j}r_{,i} - n_{,i}r_{,j})\},$$

$$V_{ijk} = (c_3/r)[(1 - 2\nu)(\delta_{ik}r_{,j} + \delta_{jk}r_{,i} - \delta_{ij}r_{,k}) + 2r_{,i}r_{,j}r_{,k}],$$

$$S_{ijk} = (c_4/r^2)\{2(dr/dn)[(1 - 2\nu)\delta_{ij}r_{,k} + \nu(\delta_{ik}r_{,j} + \delta_{jk}r_{,i}) - 4r_{,i}r_{,j}r_{,k}] + 2\nu(n_{,i}r_{,j}r_{,k} + n_{,j}r_{,i}r_{,k}) + (1 - 2\nu)(2n_{,k}r_{,i}r_{,j} + n_{,j}\delta_{ik} + n_{,i}\delta_{jk}) - (1 - 4\nu)n_{,k}\delta_{ij}\},$$

$$E_{jki} = E_{jki}^*/r = (-c_1/r)[(1 - 2\nu)(\delta_{ij}r_{,k} + \delta_{ik}r_{,j}) - \delta_{jk}r_{,i} + 2r_{,i}r_{,j}r_{,k}],$$

$$F_{ijkl} = F_{ijkl}^*/r^2 = (c_3/r^2)[(1 - 2\nu)(\delta_{ik}\delta_{jl} + \delta_{jk}\delta_{il} - \delta_{ij}\delta_{kl}) + 2\delta_{ij}r_{,k}r_{,l}] + 2\nu(\delta_{il}r_{,j}r_{,k} + \delta_{ik}r_{,j}r_{,l}) + \delta_{jl}r_{,i}r_{,k} + \delta_{ik}r_{,i}r_{,l}) + 2r_{,i}r_{,j}\delta_{kl} - 8r_{,i}r_{,j}r_{,k}r_{,l}],$$

$$f_{ij} = [-1/(8(1 - \nu))][2 d\sigma_{ij}^p + (1 - 4\nu)\delta_{ij}\sigma_{ii}^p],$$

$$c_1 = 1/(8\pi\mu(1 - \nu)), \quad -c_2 = c_3 = 1/(4\pi(1 - \nu)),$$

$$c_4 = 2\mu c_3$$

For plane stress problems, ν is replaced by $\nu/(1 + \nu)$ in the foregoing expressions. These equations are similar to those for the initial stress problems, with the initial stresses replaced by $d\sigma_{ij}^p$. Here the initial stresses refer to the stresses that exist before any elastic deformation such as the thermal or residual stresses.

3. Nonlocal continuum with local elastic strain

The essential idea of the nonlocal continuum is that some of the variables in the constitutive equation are defined by spatial averaging and only those variables which cause strain-softening are considered nonlocal while the other variables, especially the elastic strains, are still local [9,10]. In this paper, the plastic multiplier $\Delta\lambda$ in the flow rule is treated as nonlocal and is defined by the following equation

$$\begin{aligned} \Delta\bar{\lambda}(p) &= \frac{1}{V_\alpha(p)} \int_\Omega \alpha(p, q)\Delta\lambda(q)d\Omega(q) \\ &= \int_\Omega \alpha'(p, q)\Delta\lambda(q)d\Omega(q) \end{aligned} \quad (8)$$

in which

$$V_\alpha(p) = \int_\Omega \alpha(p, q)d\Omega(q) \quad (9)$$

$$\alpha'(p, q) = \alpha(p, q)/V_\alpha(p) \quad (10)$$

Here $p, q \in \Omega$, where Ω is the volume of the solid, and $\alpha(p, q)$ is the given weight function. The superposed bar refers to a nonlocal variable. The form of the normal distribution function is chosen for the weight function:

$$\alpha(p, q) = \exp(-(kr/l)^2) \quad (11)$$

where r is the distance between points p and q , l the material characteristic length which measures the degree of heterogeneity of the material, and k is a constant. $k = 2$ and 2.199 for two- and three-dimensional problems, respectively.

If the solid is finite, the normal distribution function extends beyond the boundary of the solid. This can be handled by deleting the region outside the solid from the integration domain Ω for calculating the nonlocal quantity of $\Delta\bar{\lambda}(p)$ (Eq. (8)) and for calculating $V_\alpha(p)$ (Eq. (9)). After $\Delta\bar{\lambda}$ is calculated, the spatial average values of other variables such as plastic strain increment $\Delta\varepsilon_{ij}^p$, equivalent plastic strain increment $\Delta\varepsilon_p$, and unbalanced stresses increment $\Delta\sigma_{ij}^p$ can be obtained from the general theory of plasticity [21,23] as follows:

$$\Delta\bar{\varepsilon}_{ij}^p = \Delta\bar{\lambda}a_{ij} \quad (12)$$

$$\Delta\bar{\varepsilon}_p = \Delta\bar{\lambda}(a)^T(\sigma)/\sigma_e \quad (13)$$

$$\Delta\bar{\sigma}_{ij}^p = \Delta\bar{\lambda}d_{ij} \quad (14)$$

in which $d_{ij} = D_{ijmn}a_{mn}$, σ_e the equivalent stress, and $(a)^T \times (\sigma) = a_{11}\sigma_{11} + a_{12}\sigma_{12} + a_{22}\sigma_{22} + a_{33}\sigma_{33}$ for two-dimensional cases. It is more efficient and convenient to calculate the spatial average of $\Delta\bar{\lambda}$ over plastic multiplier $\Delta\lambda$ than to have spatial average values over other quantities such as $\Delta\varepsilon_{ij}^p$ because while $\Delta\lambda$ is a scalar quantity, $\Delta\varepsilon_{ij}^p$ is a tensor that has many components.

4. Numerical implementation

After discretization of the boundary of the solid into boundary elements, Eq. (6) can be represented in a matrix form:

$$[T]\{du\} = [U]\{d\tau\} + [E]\{d\sigma^p\} \quad (15)$$

Applying the boundary conditions to Eq. (15) and rearranging it lead to

$$\{dx\} = \{dm\} + [R]\{d\sigma^p\} \quad (16)$$

Eq. (7) can also be represented in a matrix form as

$$\{d\sigma^e\} = \{dn\} + [Q]\{d\sigma^p\} \quad (17)$$

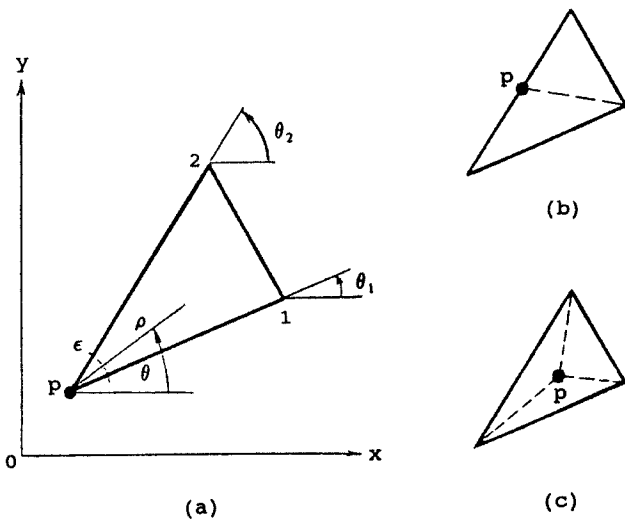


Fig. 1. Three possible singular point locations in volume integral using triangular cells.

where $\{dx\}$ is the increment of the unknown boundary displacements and/or tractions, $\{dm\}$ and $\{dn\}$ the increments of the elastic boundary solutions and internal elastic stress solutions, respectively, and $[R]$ and $[Q]$ are the coefficient matrices. It is worth pointing out that matrices $[R]$, $[Q]$ and vectors $\{dm\}$, $\{dn\}$ can be formed before the load increment procedure starts. So, it is not necessary to update these matrices and vectors during each iteration step in each load increment, which saves computer time.

In calculating coefficient matrices $[R]$ and $[Q]$, singular integrations are encountered when the volume integration is carried out over the cell that contains a singular node. These singular integrations have to be calculated properly or else an incorrect solution would result. If triangular cells with a constant interpolation function for $d\sigma_{ij}^p$ are used, there are three possible singular point locations as shown in Fig. 1(a)–(c). Cases (b) and (c) can be converted to case (a) by dividing the triangular cell into two or three sub-triangles as shown by the dashed lines in Fig. 1. For case (a), a special semi-analytical integration method similar to that used in

Telles and Brebbia [15,29] is formulated by transforming the integral to polar coordinates to avoid the singular integration:

$$\int_{\Omega_\epsilon} \frac{1}{r} E_{jki}^* d\Omega = \lim_{\epsilon \rightarrow 0} \int_{\theta_1}^{\theta_2} \int_{\epsilon}^{\rho_0} \frac{1}{r} E_{jki}^*(\theta) \rho d\rho d\theta$$

$$= \int_{\theta_1}^{\theta_2} E_{jki}^*(\theta) \rho_0 d\theta \tag{18}$$

$$\int_{\Omega_\epsilon} \frac{1}{r^2} F_{ijkl}^* d\Omega = \lim_{\epsilon \rightarrow 0} \int_{\theta_1}^{\theta_2} \int_{\epsilon}^{\rho_0} \frac{1}{r^2} F_{ijkl}^* \rho d\rho d\theta$$

$$= \int_{\theta_1}^{\theta_2} F_{ijkl}^* \ln \rho_0 d\theta \tag{19}$$

where $\rho_0(\theta) = -2A/(b_3 \cos \theta + c_3 \sin \theta)$, $b_3 = y_1 - y_2$, $c_3 = x_2 - x_1$, A the area of sub-triangle Ω_ϵ , and $E_{jki}^* = E_{jki}r$ and $F_{ijkl}^* = F_{ijkl}r^2$ are functions of θ only, without singularity. The integrations with respect to θ can then be computed using standard one-dimensional Gaussian quadrature formulas.

To calculate the nonlinear solutions by load increment procedure, Eqs. (16) and (17) are rewritten as:

$$\{\Delta x\} = \Delta\beta_k \{m\} + [R]\{\Delta\sigma^p\} \tag{20}$$

$$\{\Delta\sigma^e\} = \Delta\beta_k \{n\} + [Q]\{\Delta\sigma^p\} \tag{21}$$

where $\Delta\beta_k$ is the load increment factor at the k th step.

The Mohr–Coulomb yield surface is chosen for the yield function $f(\sigma_{ij})$ in the present study. The Mohr–Coulomb yield criterion has a yield limit that varies with the hydrostatic stress to simulate the frictional behavior of the material (Fig. 2). The so-called work hardening function $\psi(k)$ is a decreasing function with respect to k , which causes the yield surface to contract rather than expand when the material yields and starts to soften.

Based on the theory of plasticity and the hardening or softening rule, the plastic strain increment $\Delta\epsilon_{ij}^p$ can be calculated when the total strain increment $\Delta\epsilon_{ij}$ is given. Since

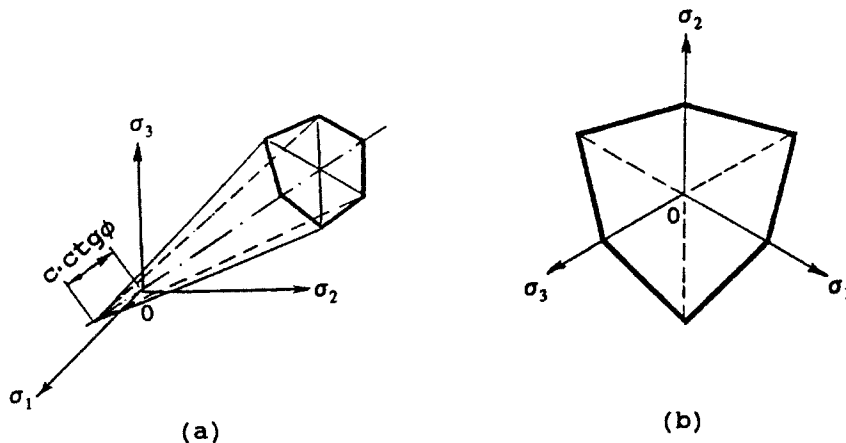


Fig. 2. Mohr–Coulomb yield criterion. (a) Geometrical presentation of yield surface in principal stress space, (b) two-dimensional representation on π plane.

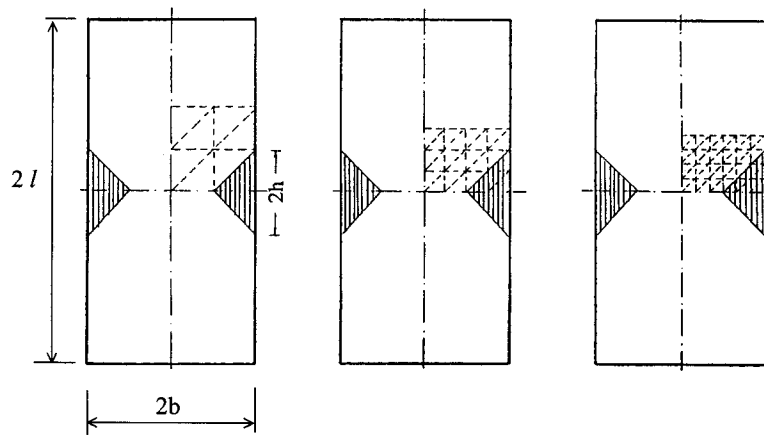


Fig. 3. Weak zones and cell mesh refinements of rectangular panel.

$\Delta\sigma_{ij}^p = D_{ijkl}\Delta\varepsilon_{kl}^p$ is not known at the beginning of each load increment, an iteration procedure must be applied. The iteration in each loading step proceeds as follows:

- (1) In the first iteration of each load increment, the prescribed traction increment or displacement increment is applied. The initial stress field is set to zero at the beginning but is not zero later on (see step 5). The elastic stress increment is calculated using Eq. (21).
- (2) Check the yield limit. For a point whose stress state lies beyond the current yield surface, calculate the plastic multiplier $\Delta\lambda$ according to the plasticity formulas.
- (3) Based on the nonlocal formulation, calculate the spatial average of $\Delta\lambda$ according to Eq. (8).
- (4) Calculate the corresponding nonlocal values of plastic strain increment, equivalent plastic strain increment, and unbalanced stresses increment according to Eqs. (12)–(14), respectively.
- (5) The unbalanced stresses computed in step 4 are treated like initial stresses and are applied to the solid in, and after, the second iteration. The prescribed tractions and displacements on the boundary are set to zero in, and after, the second iteration so that the boundary conditions would not be altered from those specified in the first iteration. After the elastic response caused by the unbalanced stresses is computed from $\{\Delta\sigma^e\} = [Q]\{\Delta\sigma^p\}$, go to step 2 to start the next iteration until the unbalanced stresses become smaller than the selected tolerance.
- (6) Go to step 1 to begin the next load increment. To avoid progressive accumulation of errors, the small unbalanced stresses left from the previous load increment are applied with the current prescribed traction and/or displacement increment.

5. Examples

A rectangular panel subjected to uniform prescribed

displacements on the top and the bottom boundaries, with the lateral boundaries free, is analyzed. The yield limit of the material in the shaded areas shown in Fig. 3 is set to be slightly less so that strain-softening would initiate at these prescribed locations. The dimensions of the panel are $l = 24$ in., $b = 12$ in. and $h = 6$ in. Linear boundary elements and triangular interior cells with constant interpolation function for $d\sigma_{ij}^p$ are used. Internal cells are employed only in the central region because strain-softening is expected to occur only in that region. Three cell meshes with different cell widths of h , $h/2$ and $h/3$ (Fig. 3) are used to study strain-softening localization. Because of symmetry, only a quarter of the rectangular panel is analyzed. The material parameters for the Mohr–Coulomb yield model used in the analysis are: Young's modulus $E = 3802$ ksi, Poisson's ratio $\nu = 0.18$, cohesion $c = 0.6675$ ksi, friction angle $\phi = 56.6$, and hardening parameter $H' = -97$ ksi. The shaded areas have the same material properties as above except that $c = 0.60075$ ksi. The characteristic length for nonlocal model is assumed to be 3 in.

Comparisons between the local and nonlocal boundary element analyses of the three meshes are shown in Figs. 4–6. Fig. 4 shows the relationship between the prescribed displacement and the reaction force induced on the top boundary. The results in Fig. 4(a) are local and those in Fig. 4(b) are nonlocal. It is found that, for local formulation, the strain-softening zone tends to localize into a band of one cell width, and that the load–displacement curves for the three meshes coincide only up to the peak loads but diverge far from each other afterward. For the present nonlocal formulation, the strain-softening zones keep the same size as the strain-softening zone of mesh 1 and the entire load–displacement curves for the three meshes are nearly identical.

The strain profiles across the strain-softening zone at the moment when the top displacement Δ reaches 0.0025 are shown in Fig. 5. For the local case, the profiles are seen to localize into progressively sharper spikes as the cell mesh is refined. For the nonlocal case, the strain profiles closely

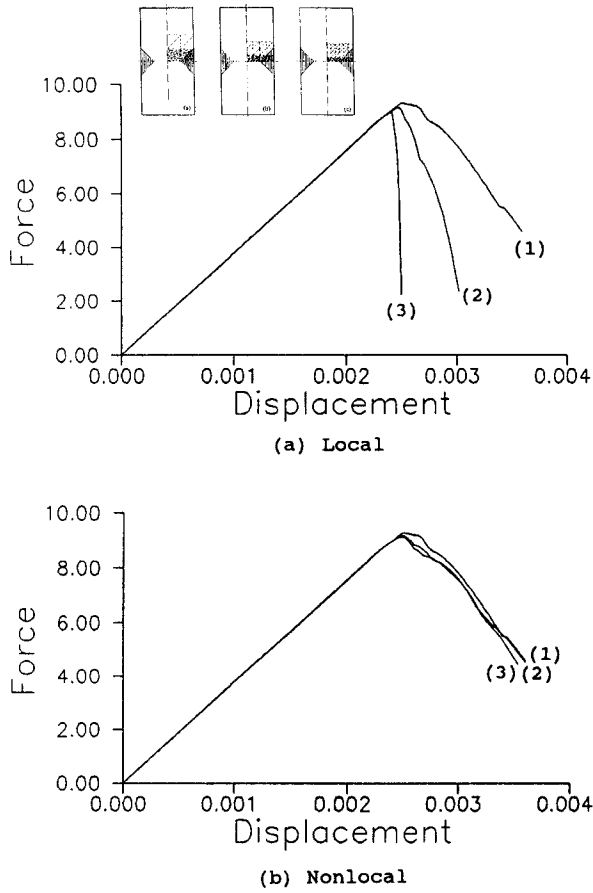


Fig. 4. Local and nonlocal load-displacement curves for the rectangular panel with strain-softening damage.

match each other for all the three cell meshes. Fig. 6 shows the total energy dissipated due to strain-softening at $\Delta = 0.0034$. The horizontal coordinate is $\log N$, where N is the number of cells in the mesh. The vertical coordinate represents the energy W dissipated in the structure. It is seen that for the local case the dissipated energy decreases with the increasing number of cells. By contrast, the energy dissipation of the nonlocal model appears to be independent of the number of cells.

It is clearly seen from the aforementioned results that the local response exhibits strong spurious mesh sensitivity even though the number of boundary elements and the material properties used in the analyses for the three cases are kept the same. The local boundary element results are not objective with respect to the cell mesh refinement. Should the mesh be refined more and more, the strain-softening zone would localize into a vanishing volume. This will lead to an incorrect conclusion that the structure would fail at vanishing zero energy dissipation.

On the other hand, the results of the boundary element analysis based on the nonlocal formulation are objective and meaningful. The nonlocal formulation eliminates the phenomenon of spurious cell mesh sensitivity and converges to a physically acceptable solution.

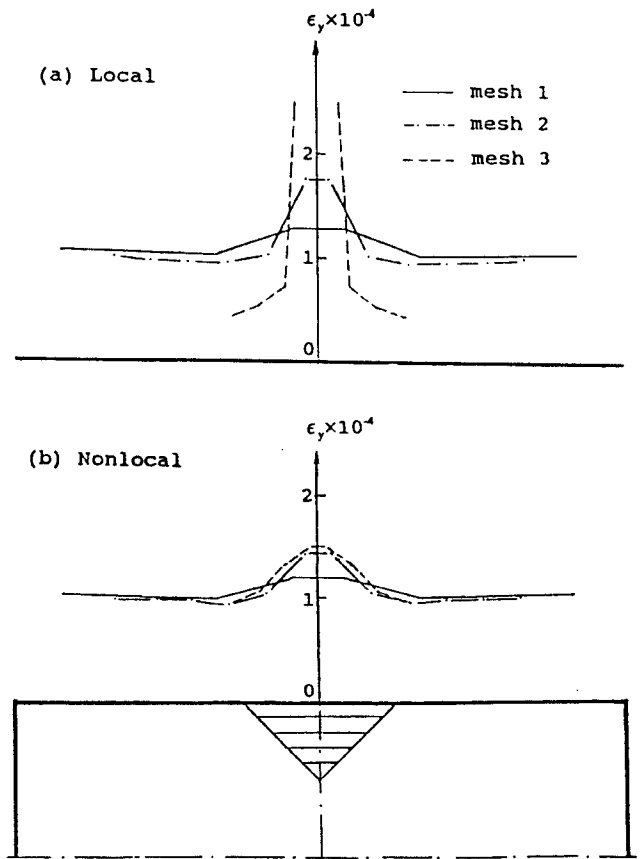


Fig. 5. Local and nonlocal strain profiles across the strain-softening zone of the three cell meshes.

For the sake of comparison, the foregoing three cases with strain hardening behavior are also analyzed. The material properties are the same as before except that $H' = 3200$ ksi. The initial weak zones in Fig. 3 are again assumed in the analysis. The results show that the nonlinear hardening zones extend all over the panel and the responses for the three cell meshes with regular local formulation are almost identical. Fig. 7 shows the load-displacement curves for the three meshes. The three curves for these meshes cannot even be distinguished from each other. This demonstrates that the localization problems are associated only with the

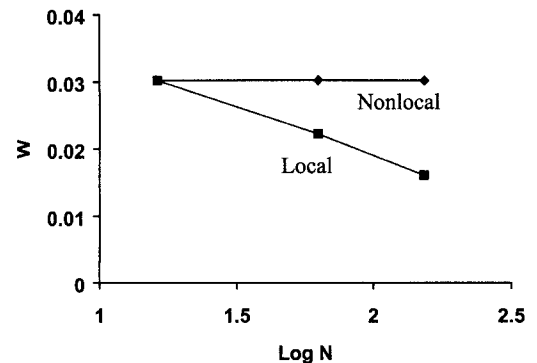


Fig. 6. Energy dissipation due to strain-softening versus number of cells.

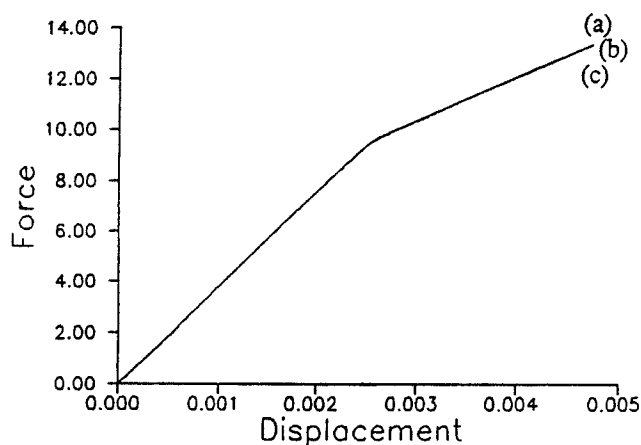


Fig. 7. Load–displacement curves for the rectangular panel with strain hardening.

strain-softening damage, which therefore, requires special treatment in order to achieve physically meaningful results.

Further examples comparing local and nonlocal solutions for another version of boundary element method are presented in Ref. [26].

6. Conclusions

1. A plasticity model with yield limit degradation is implemented in a boundary element program to study the strain-softening localization problems. The initial stress boundary element method with iteration in each small load increment is applied to deal with the nonlinear strain-softening problems. A special semi-analytical integration method is used to carry out the volume integration over the triangular cell containing a singular node.
2. Similar to the finite element analyses, the strain-softening results computed from the usual boundary element analyses (without nonlocality) are very sensitive to cell mesh refinements even though the nature of the cells is entirely different from that of finite elements. The strain-softening is found to localize into a single cell-width zone, and the energy dissipation during failure strongly depends on the cell meshes.
3. A nonlocal formulation with local strain is integrated in the boundary element program to remedy the strain-softening localization problems. A rectangular panel with three cell mesh refinements is analyzed to verify the effectiveness of the nonlocal formulation in preventing the spurious cell mesh sensitivity of the results.
4. Compared to strain-hardening plasticity problems, one of the advantages of using the boundary element method to analyze strain-softening localization problems is that the strain-softening tends to localize into a narrow band and thus the internal cells are needed only in a small region rather than the entire domain of the solid under consideration.

Acknowledgements

Partial financial support for the research under National Science Foundation Grant No. MSS-9114048 and NASA Contract No. NAG8-1561 with Polytechnic University is gratefully acknowledged. The participation of Z.P. Bažant in this study and a Visiting Scholar appointment of F.B. Lin at Northwestern University were partially supported under National Science Foundation Grant No. CMS-9713944 to Northwestern University.

References

- [1] Banerjee PK, Butterfield R, editors. Developments in boundary element methods—I. London: Applied Science Publishers, 1979.
- [2] Banerjee PK, Mustoe GG. In: Brebbia CA, editor. The boundary element method for two-dimensional problems of elastoplasticity—recent advances in BEM. London: Pentech Press, 1978.
- [3] Banerjee PK, Shaw RP, editors. Developments in boundary element methods—2. London: Applied Science Publishers, 1982.
- [4] Bažant ZP. Instability ductility and size effect in strain-softening concrete. *J Engng Mech Div, ASCE* 1976;102(EM2):331–44.
- [5] Bažant ZP. Mechanics of distributed cracking. *Appl Mech Rev, ASCE* 1985;39(5):675–705.
- [6] Bažant ZP. Nonlocal damage theory based on micromechanics of crack interactions. *J Engng Mech., ASCE* 1994;120(3):593–617 Addendum and Errata 120, p. 1401–2.
- [7] Bažant ZP, Cedolin L. Stability of structures: elastic, inelastic, fracture and damage theories. New York: Oxford University Press, 1991.
- [8] Bažant ZP, Chang TP. Nonlocal finite element analysis of strain-softening solids. *J Engng Mech* 1987;113(1).
- [9] Bažant ZP, Lin FB. Nonlocal yield limit degradation. *Int J Numer Meth Engng* 1988;26(8):1805–23.
- [10] Bažant ZP, Lin FB. Nonlocal smeared cracking model for concrete fracture. *J Struct Engng* 1988;114(11).
- [11] Bažant ZP, Lin FB, Pijaudier-Cabot G. Yield limit degradation: nonlocal continuum model with local strain. In: Owen DRJ, Hinton E, Onate E, editors. International Cont. on Computational Plasticity. Swansea: University of Wales, 1987. p. 1757–80.
- [12] Bažant ZP, Ozbolt J. Compression failure of quasi-brittle material: nonlocal microplane model. *J Engng Mech, ASCE* 1992;118(3):540–56.
- [13] Bažant ZP, Planas J. Fracture and size effect in concrete and other quasibrittle materials. Boca Raton: CRC Press, 1998.
- [14] Brebbia CA, editor. Progress in boundary element methods, vol. 1. Plymouth: Pentech Press, 1981.
- [15] Brebbia CA, Telles JCF, Wrobel LC. Boundary element techniques: theory and applications in engineering. New York: Springer, 1984.
- [16] Elfgren L, editor. Fracture mechanics of concrete structures: from theory to applications Report of RILEM TC 90-FMA. London: Chapman & Hall, 1989.
- [17] Hillerborg A. Numerical methods to simulate softening and fracture of concrete. In: Sih GC, DiTomasso A, editors. Fracture mechanics of concrete: structural application and numerical calculation. Dordrecht: Martinus Nijhoff, 1985. p. 141–70.
- [18] Hillerborg A, Modéer M, Petersson PE. Analysis of crack formation and crack growth in concrete by means of fracture mechanics and finite elements. *Cement Concrete Res* 1976;6(6):773–82.
- [19] Jirásek M. Nonlocal models for damage and fracture: comparison of approaches. *Int J Solids Struct* 1998;35:4133–45.
- [20] Lin FB, Yan G. Strain-softening damage modeling using boundary element method. In: Brebbia CA, Rencis JJ, editors. Boundary Elements XV, vol. 2. Southampton: Computational Mechanics Publications, 1993.

- [21] Mendelson A. *Plasticity: theory and application*. New York: Macmillan, 1968.
- [22] Mukherjee S. *Boundary element methods in creep and fracture*. London: Applied Science Publishers, 1982.
- [23] Owen DRJ, Hinton E. *Finite elements in plasticity—theory and practice*. Swansea: Pineridge Press, 1980.
- [24] Ozbolt J, Bažant ZP. Numerical smeared fracture analysis: nonlocal microcrack interaction approach. *Int J Numer Meth Engng* 1996;39:635–61.
- [25] Cabot P, Bažant ZP. Nonlocal damage theory. *J Engng Mech, ASCE* 1987;113(10):1512–33.
- [26] Sládek J, Sládek V, Bažant, ZP. Nonlocal boundary integral formulation for softening damage. *Int. J. of Num. Methods in Engng*. Submitted for publication.
- [27] Swedlow JL, Cruse TA. Formulation of boundary integral equations for three-dimensional elastoplastic flow. *Int J Solids Struct* 1971;7:1673–83.
- [28] Telles JCF, Brebbia CA. On the application of the boundary element method to plasticity. *Appl Math Modeling* 1979;3:466–70.
- [29] Telles JCF, Brebbia CA. The boundary element method in plasticity. *Appl Math Modeling* 1981;5:275–81.